*Journal of The Electrochemical Society*, **148** (1) C34-C40 (2001)
S0013-4651/2001/148(1)/C34/7/$7.00 © The Electrochemical Society, Inc.

# Real-Time Reactive Ion Etch Metrology Techniques to Enable *In Situ* Response Surface Process Characterization

**Pete Klimecky,*,z Craig Garvin, Cecilia G. Galarza, Brooke S. Stutzman, Pramod P. Khargonekar, and Fred L. Terry, Jr.***

*University of Michigan Electronics Manufacturing Laboratory, Ann Arbor, Michigan 48105-2551, USA*

We present a methodology termed *in situ* design of experiments (ISDOE) which enables rapid response surface design in plasma etch chambers while greatly reducing test wafer necessity. We experimentally demonstrate the ISDOE procedure on two separate systems using different optical real-time monitoring techniques to obtain wafer state data on film thickness and etch-rate estimation during reactive ion etch processes. Using the real-time wafer measurement tools during processing, we quickly obtain input/output (I/O) data to map plasma inputs to wafer outputs at multiple operating points, thereby reducing the number of test wafers necessary to obtain rich data sets for statistical model building and design of experiments. Both measurement techniques utilize *in situ* etch-rate estimations to increase the number of test set points explored per processed wafer and maximize the parameter space observed during each run. Model results and verification using these *in situ* techniques indicate no loss of accuracy when compared with traditional *ex situ* measurement methods for response surface design. Though the ISDOE concept is demonstrated here specifically on etch rate data, the general idea can be applied to many other real-time wafer state measurement methods.
© 2000 The Electrochemical Society. S0013-4651(00)01-046-6. All rights reserved.

Manuscript submitted January 13, 2000; revised manuscript received September 4, 2000.

The industrial semiconductor community widely accepts that new process development is both costly and time consuming. In particular for plasma etch processing, multiple plasma input parameters such as gas flow, pressure, and radio frequency (rf) forward power directly affect desired wafer output parameters such as etch rate, uniformity, and material selectivity. Therefore, a high number of etch experiments must be performed to accurately quantify these input and output (I/O) relationships for each process. Moreover, *in situ* wafer monitoring in general is not currently widely pursued in the industry.[1] Therefore, the typical characterization procedure can only obtain data for a single given set point per process run, where a process set point refers to the nominal input parameters used for a particular plasma condition. Thus, money and time are spent etching only one wafer for each set point required to build the input/output response surface models for a typical design of experiments (DOE). With increasing process demands and the increasing cost of larger and larger individual wafers, these test wafer costs for model design continue to become more and more acute.

This project leverages expertise from four primary research fields to achieve our results. Semiconductor process knowledge is needed to formulate the problem of new process characterization. Optical metrology background is used to obtain accurate material refractive index properties and to measure film thickness changes during processing. The thin-film properties help determine accurate film thickness and etch-rate information, which are used as inputs to the empirical process models. Nonlinear systems theory techniques are used to filter real-time optical data and estimate high speed thickness and etch-rate information. The high-speed filtering allows multiple set points to be explored per process run. Finally, response surface modeling is employed to generate empirical I/O predictions using plasma generation parameters as the model inputs, and film thickness, etch rate, and wafer uniformity as model outputs.

The goal of this research is to maximize the number of set points one can observe during a single run of the etching process by monitoring output data in real-time. This decreases the number of runs required for a complete response surface mapping, effectively reducing the number of wafers and development time required to model a new process. We show accurate and instantaneous etch-rate information (on the order of tens to hundreds of milliseconds time scales) requiring less than 100 Å of etched material;[2] therefore, we obtain empirical I/O relationships at multiple set points in a short amount of time and on a single test wafer.

In this paper, we demonstrate this *in situ* characterization mapping concept on two reactive ion etch (RIE) test-beds to show the versatility of the concept. One is an RIE chamber designed for flat panel display processing, where large area etch uniformity of an amorphous silicon (a-Si) film on metal and glass is the chosen metric for optimization. For this experiment, four independent sets of optical thickness monitoring systems, based upon laser reflectometry, were mounted at spatially distinct points above the test plate of interest. Optical measurement ports were placed radially outward from the center of the chamber as shown in Fig. 1, to monitor localized etch rates from plate center to edge in real-time. Using a nonlinear estimation technique common in systems theory called extended Kalman filtering (EKF).[2,3] we improve measurement speed and accuracy over traditional *in situ* reflectometry methods such as peak/valley counting, and we can obtain instantaneous thickness and rate information at each respective optical port. New rate data were obtained every 50 ms at each respective port, and therefore uniformity information could be instantaneously acquired from the known rates in the four zones.

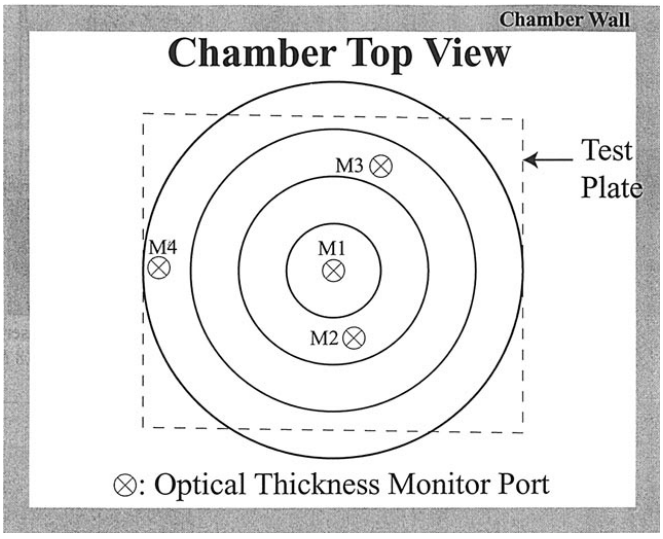


**Figure 1.** Radial position of the four local *in situ* etch-rate monitor ports.

* Electrochemical Society Active Member.
z E-mail: crown@eecs.umich.edu

For the second concept demonstration, we utilize a SOPRA[tm] real-time spectral ellipsometer (RTSE), on a commercial Lam TCP 9400SE reactor, to obtain real-time single point etch-rate information at the center of the wafer, with data collection times of 180 ms. [4] We use the RTSE to rapidly map and characterize polysilicon etch rates across a range of variations on a standard Lam main etch process recipe.

This paper details experimental verification of such a rapid modeling methodology using two validation methods. For the first experiment, we compare predictions made by the model built using *in situ* data, with *ex situ* measurements at process points not explicitly explored by the original experimental design. One such process set point lies extrapolated just outside the empirically modeled process space, while a second lies interpolated just inside the process space explored by the original DOE. For the second experiment, we compare multiple runs at the same set of conditions, but with process run order changed to confirm there is no loss of model accuracy from step sequence position imposed by the *in situ* DOE method (ISDOE).

## ISDOE Concept

The difference between common response surface model building and our ISDOE method lies in the measurement technique used to acquire the data at the requisite operating points. Conventional quantitative mapping between plasma input parameters and output wafer characteristics explores the response surface of the process space, defined by the DOE statistical technique, using post-process thickness measurements of a single sample at a single operating condition. DOE statistical modeling has been shown to accurately characterize the process space of interest.[5] The typical model building procedure starts with a set of initial operating conditions for plasma inputs and maps the resulting wafer parameter outputs to create a purely empirical I/O design. The resulting model is then tested at specific new operating points, and the prediction is compared to measurement. If the prediction errors are unacceptable, the model is refined with further data collection until the model appropriately matches measurement. Our methodology does not modify these statistical principles but rather the way in which the data sets are obtained. Traditional DOE is an effective modeling procedure; however, the time and cost requirements of multiple experiments can become extensive when many runs are required for high-accuracy models. Of particular importance to the semiconductor industry, the overall cost of a conventional DOE procedure is typically proportional to the cost of each individual process run and test wafer required to obtain the model database.

By contrast, our ISDOE method greatly reduces the number of runs needed for model building by obtaining accurate output data at multiple operating conditions on each wafer. In this procedure, several set points are implemented per run, thereby decreasing the overall cost of the modeling task without decreasing model accuracy. In addition, repeated tests for refined model accuracy, as well as expanded process space mapping, also benefit greatly from *in situ* metrology by enabling one to acquire richer data sets more quickly.

Two issues with the *in situ* DOE method need to be addressed in order to obtain a valid measurement data set as compared with traditional methods. First, we need reliable, stable, and accurate *in situ* wafer state estimates (in this case etch-rate estimates) at each set point condition during the run. This means both that process transients must settle out to steady state between process steps, and the wafer state metrology data must converge and stabilize within acceptable bounds. Second, there must be no process drift from the start of the experiment to the end, nor any hysteresis or ordering effects of the sequence in which the process steps were made. If these conditions are all met and carefully monitored, the ISDOE yields sufficiently accurate parameters for comparative model building. Here we show results of two *in situ* measurement techniques to facilitate the implementation of the ISDOE strategy as effective tools for rapid model development.

For both the dual-wavelength reflectometry technique and the RTSE-based experiments, the key enabling mechanism toward maximizing the observable process space per etched wafer is the accurate real-time thickness estimation. The former method is well suited for the a-Si case due to the relative simplicity of the material stack, and therefore the ease with which the EKF estimation can track thickness and etch rate simultaneously at all four ports. These factors made *in situ* uniformity characterization tractable. The inherent complexity of the polysilicon stack, however, made the latter method a more attractive choice for monitoring real-time rate estimation for that case.

## Plasmatherm Experimental Details

For the first experimental setup, we studied rapid uniformity modeling on a PlasmaTherm Clusterlock 7000 RIE chamber designed for large-area flat panel etching. Each plate is 350 × 400 mm. For this system we chose an HCl gas chemistry, which is a new process for this chamber, with unknown etching uniformity characteristics. Such a new process assures no *a priori* knowledge bias on the chosen process regime we are to model. Commanded inputs are pressure, rf incident power, and HCl gas flow rate, where the outputs were the localized etch rates and corresponding etch uniformity. Using four sets of dual-wavelength reflectometry systems and the EKF estimation technique, we monitored the etch rate at four distinct points on a plate in real-time. The objective of the DOE was to improve the etch-rate uniformity defined as $U = \mathrm{ER}_{max} - \mathrm{ER}_{min}/\mathrm{ER}_{min}$ between the four respective ports, where $\mathrm{ER}_{max}$ represents the etch rate for the local port with the highest rate and $\mathrm{ER}_{min}$ represents the lowest rate location. With the EKF technique, we were able to obtain five different set points per plate, as opposed to a conventional method which would achieve one I/O set point by *ex situ* measurement. We constructed a model with ten samples of the response surface, thus reducing the required test plates to only two. The model was then validated on two separate set points, one inside and one outside the modeled parameter space, using a more traditional *ex situ* spectral reflectometer measurement for comparison. The two-plate ISDOE database is summarized in Table I, where etch rates are listed in angstroms per second.

The primary source of error in these etch-rate measurements is due to potential inaccuracies in the complex refractive index parameters (N, K) for the a-Si film. N, K values for this film were estimated using off-line spectral ellipsometry (SE) analysis. However, though systematic errors in the extracted N, K values may affect absolute values in film thickness (and therefore etch rate), the final uniformity results used in the DOE are not largely influenced by refractive index inaccuracies, since the uniformity metric is based on a relative difference between localized etch rates at respective ports. The reproducibility of these etch-rate measurements is on the order of a few angstroms, and there is good agreement between the on-line EKF measured data and off-line film measurements. Taking these points into consideration, we expect the final uniformity results for this experiment to be accurate to within 5% using this *in situ* technique.

The experimental setup shown in Fig. 2 couples monochromatic light from a red HeNe laser at 632.8 nm and a green diode laser at 532 nm into one bundled multileg fiber optic cable. Both input beams

**Table I. 10 pt, two-sample, *in situ* DOE etch rate data.**

| Pressure (mT) | Power (W) | HCl flow (sccm) | ER1 | ER2 | ER3 | ER4 | Uniformity (%) |
|---|---|---|---|---|---|---|---|
| 40 | 300 | 300 | 3.343 | 3.64 | 4.47 | 4.245 | 33.70 |
| 20 | 200 | 200 | 2.583 | 2.521 | 2.823 | 3.148 | 24.87 |
| 20 | 400 | 200 | 3.586 | 3.922 | 4.399 | 4.758 | 32.68 |
| 20 | 400 | 400 | 2.88 | 6.153 | 7.004 | 7.234 | 23.03 |
| 60 | 200 | 400 | 1.453 | 1.643 | 2.041 | 2.309 | 58.91 |
| 40 | 300 | 300 | 3.56 | 3.834 | 4.696 | 4.906 | 37.81 |
| 20 | 200 | 400 | 2.529 | 2.600 | 3.088 | 3.415 | 35.03 |
| 60 | 400 | 400 | 4.05 | 4.372 | 5.679 | 5.918 | 46.11 |
| 60 | 200 | 200 | 1.43 | 1.504 | 1.989 | 2.148 | 50.22 |
| 60 | 400 | 200 | 3.184 | 3.605 | 4.558 | 4.729 | 48.52 |

are modulated by separate mechanical choppers at different frequencies to help reduce unwanted noise. A beam diffuser at the fiber input assures stable light intensity is delivered into each leg of the fiber. Each fiber leg attaches to a collimating beam probe and couples to one of four beam-splitting cubes on top of the RIE chamber to reflect input light from the sample surface at normal incidence. Light is reflected through the respective beam-splitting module, is collimated, and then couples into a receiving fiber at a right angle to the incident beam. Reflected light from each port is incident upon a photodiode detector to determine intensity, and the converted signal is passed to a lock-in amplifier tuned to the respective red and green chopper frequencies. Proportional signals from the lock-ins are recorded as individual signals by an automated computer data acquisition system running LabVIEW$^{tm}$.[6] In this experiment, four unique optical ports are monitored across the sample surface, each reflecting red and green light intensities, and thus four photodiodes are required, one for each port. With both red and green signals, therefore, eight inexpensive lock-in amplifiers are required to read both laser intensities at each port, plus an additional two lock-ins to record and account for incident beam intensity and possible variations.

The basic concept used for the dual-wavelength reflectometry is well known; however, we employ a new EKF filtering technique to increase measurement speed and accuracy. Laser light is introduced at normal incidence and the detector is aligned for maximum reflected signal intensity at the beam-splitting module. During processing, as the sample material is etched, the reflected light intensity changes periodically through constructive and destructive interference. At each instant in time, the reflected light intensity can be described by a well-known optical model as follows[7]

$$I_r[d(t), \lambda] = I_0 r[d(t), \lambda, N] \quad [1]$$

where $I_r[d(t), \lambda]$ is the reflected light intensity, $d(t)$ is the thickness at time $t$, $\lambda$ is the incident wavelength, and $N$ is the refractive index of the thin film. Note, however, that Eq. 1, represents a relative intensity change to the incident beam. In reality, we measure an absolute intensity change and not a relative intensity, which is more accurately modeled as

$$I_r[d(t), \lambda] = \gamma I_0 r[d(t), \lambda, N] + \delta$$

where $\gamma$ is the gain in the optical system and $\delta$ is the offset value, respectively, both of which are characteristic of the optical ports, beam alignment, and measurement station at the time of the measurement.

Traditional reflectometry is typically limited to 1/4 wavelength accuracy, or at least one peak/valley transition to obtain valid thickness information. However, we employ a novel approach to improve the accuracy and speed with which to obtain thickness and etch-rate information from the reflected light intensity which can converge to accurate etch rate estimates much faster than 1/4 wave thickness changes. Utilizing the technique developed in Ref. 3, we are able to obtain fast and accurate *in situ* etch-rate measurements using an EKF to process the reflected light data. The EKF is an efficient technique for performing nonlinear estimation,[8] and it allows one to deduce highly accurate etch-rate information from the thickness information contained in the absolute light intensity variations. An EKF can be designed to estimate the value of $d(t)$ and its derivative $\dot{d}(t) = e_r(t)$ [8] at each discrete instant in time. Prior to each run, an independent *ex situ* film thickness measurement is obtained via a traditional method such as spectrophotometry (SP) to seed the EKF algorithm with an initial thickness. An absolute intensity measurement is also made using a highly reflective aluminum sample to help define the gain and offset values for the EKF for each run. To ensure a rapid convergence of the estimation algorithm and to account for uncertainties in the initial thickness measurements, the software algorithm runs many EKFs in parallel using slightly different initial thickness values. The number of filters run at once is defined by the user for each run, in order to include the range of uncertainty in the starting film thickness. The final etch-rate estimation is obtained as a weighted average of each individual estimation. For the a-Si film stack under this study, it suffices to say that this setup allows us to obtain very accurate instantaneous etch-rate measurements, primarily due to the well-defined optical characteristics of a-Si. As quoted in Ref. 9, the accuracy of these measurements has been previously verified to be typically within 15 Å of off-line SE measurements, where the SE measurements are expected to have 1-2 Å accuracy. Although the data was collected in real-time at deterministic intervals, analysis for these experiments was performed off-line for greatest accuracy of the EKF. On-line analysis is possible, however, and has been demonstrated in Ref. 9. For a detailed explanation of the actual EKF algorithm, we refer the interested reader to Ref. 2 and 3.

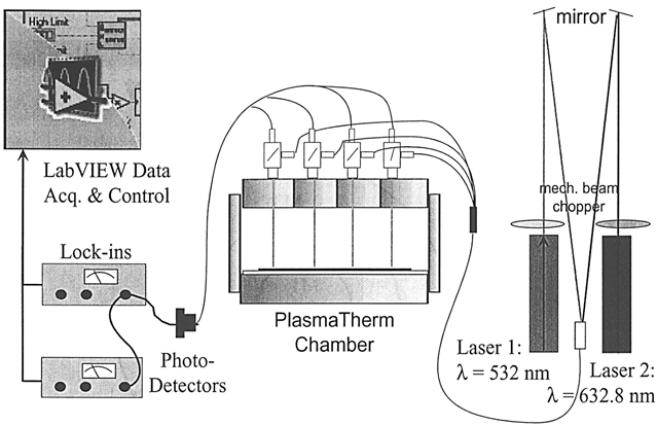


**Figure 2.** Four-zone, dual-wavelength thickness and etch-rate monitor system.

## Plasmatherm Results

The etch rates (in angstroms per second) and etch uniformity predicted by the model are very accurate at the first validation set point as shown in Table II. The maximum relative etch rate error is 5.5%, and the etch uniformity differs by 7.1% from the prediction made by the model. Standard *ex situ* thickness measurements made with a Leitz MPV-SP spectrophotometer showed only up to a 3.5% discrepancy between prediction and measurement, demonstrating no loss of accuracy using this *in situ* DOE method.

Etch rates at each port were modeled using the following form

$$ER = \alpha_1 + \alpha_2 \text{Pressure} + \alpha_3 \text{Power} + \alpha_4 \text{Power} \times \text{Flow} \quad [3]$$

where $\alpha_1$, $\alpha_2$, $\alpha_3$, $\alpha_4$ are constant coefficients that depend on the location of the optical port. These coefficients were obtained by solving a least-squares regression. Data used to obtain this rate model are summarized in Table I.

We validated the *in situ* rate model at two new set points, run independently, where the verification data is obtained via traditional post-process measurement for comparison. These rates are compared with the model prediction in Table II, where etch rates at each port are again quoted in angstroms per second. The column labeled "Model" represents the predicted mean etch rate at each port and the corresponding overall rate uniformity. The "SP" column lists the post-process thickness measurements made by a microscope-based spectral reflectometer (SP) at the beginning and end of the run, yielding the average rate taken over the course of the etch. Note that the SP

**Table II. Validation runs for *in situ* DOE using the dual-wavelength method.**

| | Verification 1 | | Verification 2 | |
|---|---|---|---|---|
| | Model 1 | SP1 | Model 2 | SP2 |
| ER1 | 4.49 | 4.52 | 6.54 | 6.38 |
| ER2 | 4.75 | 4.65 | 6.96 | 6.62 |
| ER3 | 5.54 | 5.35 | 8.19 | 7.52 |
| ER4 | 5.83 | 5.66 | 8.46 | 7.96 |

method is a standard means of obtaining etch-rate data, while the model was developed by the new EKF method of post-processing the *in situ* reflectometry data. SP measurement accuracy for these films was typically in agreement with SE measurements to within 20 Å, where again, the SE measurements are expected to have 1-2 Å accuracy. SP reproducibility is within a few angstroms for these films.

Our first verification set point is inside the modeled process space at 25 mT, 360 W, and 350 sccm HCl flow, and it demonstrates a good rate agreement at each port, all within 3.5%, between the traditional *ex situ* SP etch-rate measurement and the model prediction based upon *in situ* data. The uniformity prediction also agrees with SP data within 4.3%. Therefore, we conclude there is no loss of accuracy in the model using the ISDOE method described. The second set point at 22 mT, 495 W, and 400 sccm HCl flow lies just outside the process space explored by the DOE, but in a regime which the model suggests may yield a higher uniformity metric than other previously measured operating conditions. Due to the simple, empirical nature of the model and the complexity of the plasma process, we would expect this second verification point to not agree as well as the first, but still hopefully show an improvement in uniformity. Indeed, the individual etch rate estimates have roughly twice the error as those within the modeled space regime, ranging from a 2.4 to 8.1% difference, but the uniformity prediction remains reasonably accurate with a 2.6% discrepency. Actual uniformity improvement at the new verification point appears negligible, so we can conclude that a range of processing points in this area of the modeled space should yield similar results. These results are in line with previous model agreement when tradition DOE procedures were used. Overall, the modeled prediction *vs*. actual post-process measurement appears to be in close agreement and suffered no loss of accuracy using the *in situ* measurement tool to obtain the response surface.

The primary limiting factors for how many I/O pairs can be mapped per sample depend upon the combination of initial thickness of the film, the wavelengths of the light used, the rate of convergence of the EKF algorithm, and the process parameter settling time between steps. Clearly, one wishes to maximize the initial film thickness so that more material is available for etching and therefore more set points can be explored. However, the monochromatic laser light undergoes too much absorption in thick films to reflect a quality signal, and therefore maximum film thickness is limited. The shorter the wavelength, the thinner the film required for an acceptable reflected signal. In our case, the green laser at 532 nm became too highly absorbed for films thicker than roughly 2500 Å, therefore, we used initial a-Si samples in the 2500-3000 Å range. The second factor is the time required between process steps for the plasma inputs to stabilize to the new values, and consequently, the time required for the EKF to converge to a steady-state etch-rate estimation. Typically for our experiments, we found anywhere from 100 to 500 Å needed to be etched to obtain steady, well-averaged, quality etch-rate data, and thus starting at ~2500 Å we conservatively chose to etch five set points on each sample.

Thus, the ISDOE method for this experiment measured ten set points using only two samples. Representative plots of the plasma input step changes as they can affect pressure, and the corresponding etch-rate changes are shown in Fig. 3. This plot represents five respective operating points explored on a typical ISDOE run, and it is shown here to emphasize that input transients between set point values are allowed to settle out before estimating etch rates for the DOE model at a given condition. This plot shows more exaggerated transients than those seen for the two test runs presented in this paper, so as to better demonstrate the technique. Steady-state etch rates were established for the response surface characterization once all step input transients had dissipated and the EKF algorithm had converged to an acceptable tolerance. Figure 4 shows the respective raw red and green wavelength reflected laser signals as they change in periodicity at each new step in the process, demonstrating new etch rates for each operating point during the run.

It should be noted that although this experiment was performed on blanket film structures, the concept does not necessarily exclude similar techniques being employed on patterned structures in the future. Work on rate estimations using either scalar diffraction analysis for larger pattern structures, vector diffraction methods for smaller structures [such as the rigorous coupled wave analysis (RCWA)], or perhaps algorithms combining the two techniques, is currently under investigation.[10-16] The time scales for patterned structure analysis are undoubtedly longer than presented here, but the time limitations may be possible to decrease to a level where the ISDOE concept could be employed to an advantage over traditional DOE methods.

### ISDOE Experiments on Lam 9400

In this section, we present the fit and prediction of multivariate regression models relating process inputs of pressure, power, and gas flow rates to polysilicon etch rate inferred from the RTSE measurement. A two-level experiment in five factors, illustrated in Table III, is used. Employing a Plackett-Burman experimental design enables five factors to be spanned in 16 set points with no confounding among first-order interactions.[17] Each 150 mm polysilicon wafer, with 5000 Å initial poly thickness, was etched and monitored at four distinct set point conditions, respectively. In order to assure a con-

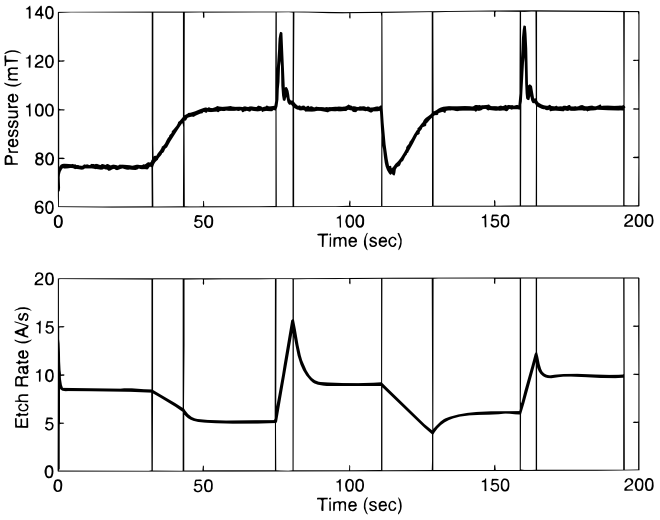


**Figure 3.** Representative implementation of five set points during one test sample run.

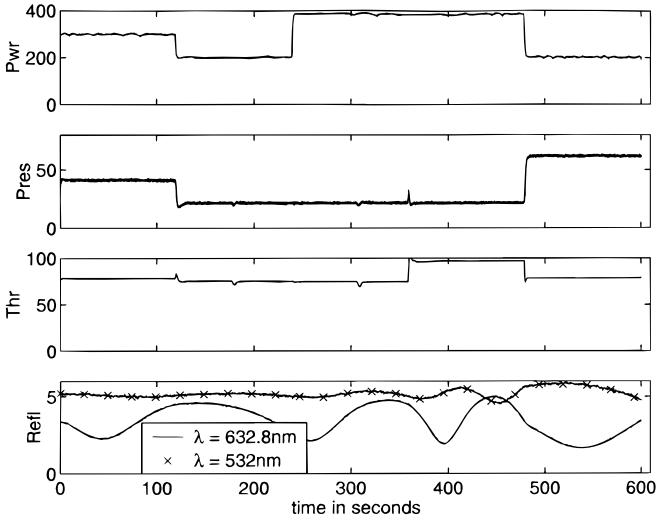


**Figure 4.** Raw laser data: rate changes at each process step in run. Pwr = plasma input power (W), Pres = chamber process pressure (mT), Thr = chamber throttle valve position (% open), Refl = scaled photodiode level for respective laser (0-10 V).

**Table III. Experimental variables and levels.**

| Level | Pressure (mTorr) | Bias (W) | TCP (W) | $Cl_2$ (sccm) | HBr (sccm) |
|---|---|---|---|---|---|
| Low | 10 | 100 | 300 | 25 | 25 |
| High | 25 | 225 | 450 | 100 | 100 |

stant, stabilized poly etch-rate estimation for each new set point, we chose to average over 600-800 Å of etched material before stepping to the next condition, resulting in approximately 15 s of etching at each new point. Therefore, we were able to run four separate points per wafer before our 5000 Å poly stack was depleted. Each set point is repeated five times over the four set points explored with each etched wafer. The result is that 20 wafers are required to perform 80 experiments in random order. To determine the impact of relative order within the etch on etch rate, the relative order (1-4) of each experiment is logged. The experimental data is separated into a model development set composed of four repetitions of the set points and a model testing set comprising the remaining repetition. The regression analysis is performed on all five combinations of development and testing set, and results are presented as an average of the five combinations.

*Lam experimental setup.*—This second experiment qualified polysilicon etch rate on a Lam 9400SE reactor under various plasma conditions. Due to the inherent surface roughness characteristics of polysilicon which makes the refractive index difficult to model, a more sophisticated real-time measurement tool was chosen for this project. We selected a commercial SOPRA RTSE to monitor polysilicon etch rates. A minimal and nonintrusive modification to the lower chamber ring of this otherwise stock commercial chamber was made to facilitate inclusion of stress-free optical ports mounted on opposing sides for ellipsometric measurements at a fixed incident angle of 63.5°. These windows allowed monitoring of center wafer thickness during processing.

The RTSE records the ellipsometric angles, $\tan(\Psi)$ and $\cos(\Delta)$, at a fixed angle of incidence with a rotating polarizer frequency of 11 Hz, and new data is processed and collected every 180 ms, as depicted in Fig. 5. Full spectral white light from a Xe arc lamp is reflected from the wafer surface and binned into 512 distinct wavelengths on a photodiode array detector, ranging from 257.8 to 687.5 nm and acquired in real-time. Thickness and etch rate information is then modeled off-line using a Bruggeman effective media approximation (EMA) for the surface roughness layer. The film layers are modeled as the EMA layer on less than 5 kÅ poly on 300 Å $SiO_2$ on Si(100) substrate, as shown in Fig. 6. However, this surface model is an imperfect estimation leading to a common systematic error in the measurement of the bulk poly refractive index at each wavelength, $N(\lambda)$.[18] Therefore, typically somewhat more material needs to be etched in order to obtain quality etch-rate data for use in the response surface model. Random errors in the thickness estimation, however, can be reduced with fast sampling compared to the etch rate. If we assume the measured thickness value is

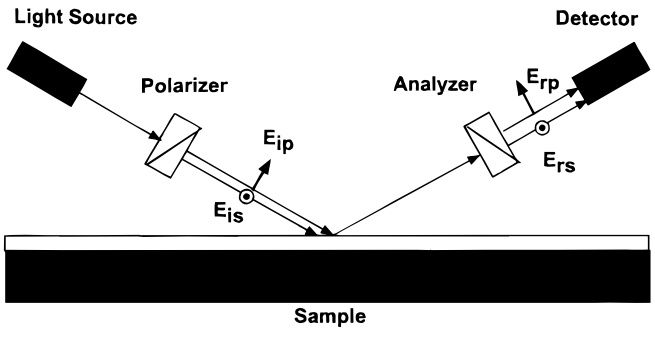


**Figure 5.** Real-time spectroscopic ellipsometry.

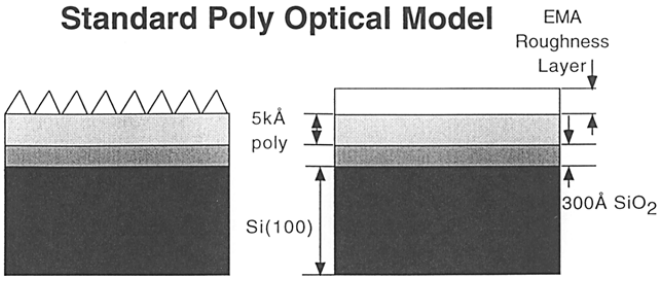


**Figure 6.** Polysilicon film stack model using Bruggeman EMA.

$$\hat{d} = d_{\text{actual}} + \delta d_{\text{random}} + \delta d_{\text{systematic}} \quad [4]$$

and therefore the measured etch rate is

$$\hat{E} = \left[\frac{\hat{d}(t_{i+1}) - \hat{d}(t_i)}{\Delta t}\right] \quad [5]$$

Then we can reduce the random effects by fast and accurate sampling since $\delta d_{\text{sys}} = 0$

$$\Delta d = E\Delta t = \sqrt{2}\left(\frac{E}{\sigma_e}\sigma_d\right) \quad [6]$$

However, the systematic error caused by the ill-defined refractive index of the surface roughness simply requires further etched material and rate estimation averaging for accurate results. We typically needed 600-800 Å of etched material for accurate rate information. Thickness and corresponding etch-rate data using this approach are shown in Fig. 7. Here, the left axis (black) plots the real-time change in polysilicon thickness, while the right axis (gray) shows the corresponding etch-rate estimations at each set point in nanometers per second. Etch rate is simply the slope of the thickness plot. It should be emphasized that the thickness limitation mentioned is due to the optical modeling problem and not the accuracy of the RTSE or any limitation inherent to the ISDOE concept.

*Experimental analysis.*—Our analysis approach is to regress a model, *B*, using the model development set, and evaluate its fit on this set, as well as its predictive capabilities on the model testing set, as shown in Eq. 7-9. *X* represents the process inputs, and *Y* represents the dependant variable of etch rate. Standard font, [*X*, *Y*], represents elements of the model development set, while script font, [$\mathcal{X}$, $\mathcal{Y}$], represents elements of the model testing set. Capital letters,

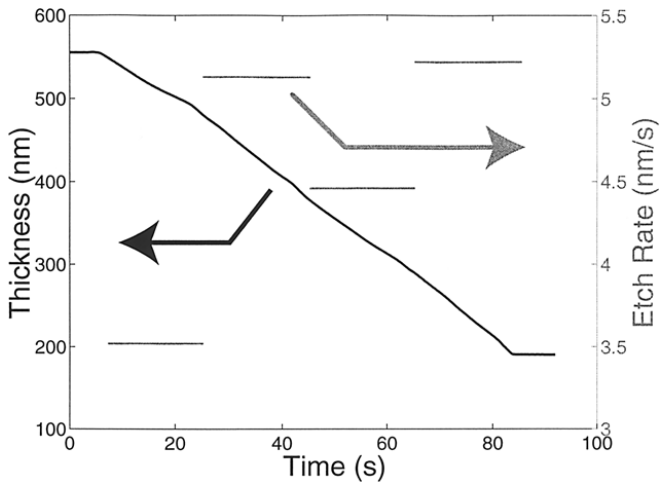


**Figure 7.** Polysilicon etch-rate estimates for each step during a run.

*X*, represent all process inputs, while lower case, *x*, represents a single process input

$$\hat{Y} = XB \quad [7]$$

$$\hat{\mathcal{Y}} = \mathcal{X}B \quad [8]$$

$$B = (X'X)^{-1}X'Y \quad [9]$$

Although the experiment is in five input factors, the output can be a linear function of 16 variables: a mean term, the five factors, and ten first-order interactions. Given this sizeable choice of variables from which to form a model, the challenge, as is often the case,[19,20] is subset selection. Accordingly, we use a stepwise regression[21] with an F test[22] to determine model order and constituents.

Since the maximum model order is smaller than the number of experiments, we begin with a model using all 16 factors and interactions and order it, using the iterative algorithm shown in Eq. 11-14

$$X_i^{\text{temp}} = [x_1 \cdots x_{i-1}x_{i+1}\cdots x_j] \big| x \in X_j^{\text{ord}} \quad [10]$$

$$E_i = \|Y - \hat{Y}_i\|_2 \quad [11]$$

$$\hat{Y}_i = X_i^{\text{temp}}[(X_i^{\text{temp}})'X_i^{\text{temp}}]^{-1}(X_i^{\text{temp}})'Y \quad [12]$$

$$X_{j-1}^{\text{ord}} = X_{i\star}^{\text{temp}} \quad [13]$$

$$i^\star = \text{ARG}[\min(E_i)] \quad [14]$$

We initialize $X_j^{\text{ord}}$ = all 16 factors and $j = 16$. We form $j$ $X_i^{\text{temp}}$'s, each missing the *i*th variable. The variable $x_{i\star}$ is the component of $X_j^{\text{best}}$ that least contributes to fitting *Y*. Accordingly, $X_{j-1}^{\text{ord}}$ is formed from $X_j^{\text{ord}}$ by eliminating $x_{i\star}$. Once the process is repeated to $j = 1$ the result is a set of variables ordered by their ability to predict *Y*.

Having ordered the sensor variables, it is clear that at some point, improvement in fit on the model development set is no longer significant. A standard formalization of this observation is the use of an "F test" on different sized models. Given two models of size *n* and *m*, $n > m$, and the mean squared error, $E_n$ and $E_m$, achieved using models of size *n* and *m*, the F test gives the likelihood that the reduction in error is due to chance. We can apply the F test to models based on $X_j^{\text{ord}}|_{j=1}^{16}$. Once the probability that the improvement from $X_{j+1}^{\text{ord}}$ to $X_j^{\text{ord}}$ is due to chance greater than 5%, we determine that the best model size has been reached.

The combination of ordering and F test gives a sound basis for the focus of this investigation: the impact of the ISDOE procedure on model performance. In addition to unknown variations from run to run, repetitions of the ISDOE vary by relative order within an etch. We propose two ways of evaluating the impact of relative order. First, we compare the model fit on the modeling set to model prediction on the test set. If both are qualitatively very good, then the impact of relative order can be considered minimal. An additional test involves using the relative order to fit the residual error. The residual error is that part of the etch rate that is not modeled by the process inputs. Clearly, if relative order of the set point is correlated to this residual, then relative order may be a factor in the experiment. Conversely, if the two are not correlated, then relative order clearly is not a factor and the experimental results support the ISDOE approach.

*Lam experimental results.*—The method described in the preceding section is applied to all five permutations of test and model sets. Average results are shown in Table IV. As the name indicates, the fit on the modeling set reflects the $R^2$ performance of the model on the data used to develop the model. Likewise, the prediction on the test set is the $R^2$ performance of the model on data not used for model development. In all five permutations of test and model set, the same model order resulted. Applying the F test described in the previous section resulted in only two of the set of 16 potential variables being eliminated as statistically insignificant. The final model includes the mean, all five main effects, and all interactions except those between power and HBr (TCP × HBr, Bias × HBr).

**Table IV. Experimental variables and levels.**

| $R^2$ fit, modeling set | $R^2$ prediction, test set | Model order |
|---|---|---|
| 0.9579 | 0.9308 | 14 |

The results in Table IV support the ISDOE approach. The fit is extremely good and prediction is very good. The accuracy of the empirical model certainly suggests that the impact of relative order within the etch is small and that the assumptions underlying ISDOE are validated.

The ISDOE approach is further supported by analysis of residual error. The best fit of relative order to residual error achieves an $R^2 = 0.0168$ with a fourth-order polynomial in relative order. Essentially, there is no correlation between the two, and thus, whatever the cause of run-to-run etch-rate variation, it is clearly not order within the etch.

The results of this experiment are clear in their support of the ISDOE approach. Not only is the predictive ability of the model nearly as good as its fit, none of the model error can be explained by the additional feature of the ISDOE approach, which is that set points are run for portions of a wafer etch rather than the total duration.

## Conclusions

The ISDOE method has been shown, using etch rate information, to reduce the number of test wafers required for response surface design experiments without compromising model performance, thus improving machine utilization. The key enabling technology for the particular model building approach demonstrated here for RIE systems is a real-time *in situ* thickness monitoring capability on test samples. Two such techniques, a dual-wavelength reflectometry system and a SE system, have been demonstrated, and the resulting models compared favorably with experimental etch data. We believe this ISDOE concept may be applied to various process modeling applications, yielding the rapid mapping of new processes and reduced test wafer costs in terms of both time and money savings. For example, *in situ* uniformity in some systems could be done with imaging techniques such as LES or full wafer interferometry.[23-25] More advanced wafer state data, such as *in situ* CD/wall angle using SE[10,13-15] could lead to more advanced ISDOE implementations. Other wafer state measurements might include temperature uniformity tuning using IR sensing or plasma mapping using spacially resolved optical emission spectra.[26]

## Acknowledgments

This work was supported in part by AFOSR/ARPA MURI Center under grant no. F49620-95-1-0524 and the Semiconductor Research Company under contract no. 97-FC-085 and the State of Michigan.

*The University of Michigan Center for Integrated Microsystems assisted in meeting the publication costs of this article.*

## References

1. E. A. Rietman, D. E. Ibbotson, and J. T. C. Lee, *J. Vac. Sci. Technol.*, **B16**, 131 (1998).
2. T. L. Vincent, P. P. Khargonekar, and F. L. Terry, Jr., *Mater. Res. Soc. Symp. Proc.*, **10**, 87 (1996).
3. T. L. Vincent, P. P. Khargonekar, and F. L. Terry, Jr., *IEEE Trans. Semicond. Manuf.*, **SM-10**, 42 (1997).
4. B. S. Stutzman, H. M. Park, P. Klimecky, C. Garvin, D. Grimard, D. Schweiger, and F. L. Terry, Jr., Abstract 263, The Electrochemical Society Meeting Abstracts, Vol. 99-1, Seattle, WA, May 2-6, 1999.
5. D. C. Baird, *Experimentation: An Introduction to Measurement Theory and Experiment Design*, Prentice-Hall, Englewood Cliffs, Nj (1995).
6. P. Klimecky, D. Schweiger, and J. Grizzle, Abstract 214, The Electrochemical Society Meeting Abstracts, Vol. 99-1, Seattle, WA, May 2-7, 1999.
7. R. Azzam and N. Bashara, *Ellipsometry and Polarized Light*, North Holland, New York, NY (1989).
8. B. Anderson and J. Moore, *Optimal Filtering*, Prentice-Hall, Englewood Cliffs, NJ (1979).
9. T. L. Vincent, P. Klimecky, W. Sun, P. P. Khargonekar, and F. L. Terry, Jr., *Proc. Int's Display Res. Conf., IDRC97*, Toronto, Ontario, Canada, Sept 1997.
10. X. Niu, N. Jakatdar, Bao, J. C. Spanos, and S. Yedur, *Proc. Spie-Int. Soc. Opt. Eng.*, **3677**, 159 (1999).
11. H. L. Maynard, N. Layadi, and J. T. C. Lee, *Thin Solid Films*, 314/315 (398), (Feb 1998).

12. C. Galarza, P. Khargonekar, and F. L. Terry, Jr., in *Proceedings of the 1999 IEEE International Conference on Control Applications*, Vol. 1, p. 773, IEEE, Piscataway, NJ (1999).
13. M. E. Lee, W. Galarza, C. Kong, W. Sun, and F. L. Terry, Jr., in *International Conference on Characterization and Metrology for ULSI Tech*, Gaithersburg, MD, Vol. 449, p. 331, AIP Conference Proceedings, March 1998.
14. H. Huang, W. Kong, B. Stutzman, and F. L. Terry, Jr., in *Proceedings of SEMATECH AEC/APC Symposium*, Vail, CO, Sept 1999.
15. H. Huang, W. Kong, H. Kim, W. Sun, and F. L. Terry, Jr., Abstract 244, The Electrochemical Society Meeting Abstracts, Vol. 99-1, Seattle, WA, May 2-6, 1999.
16. B. S. Stutzman, W. Kong, H.-T. Huang, and F. L. Terry, Jr., Abstract sc08.09, American Physical Society Centennial Meeting, Atlanta, GA, March 1999.
17. R. L. Plackett and J. P. Burman, *Biometrika*, **33**, 305 (Feb 1946).
18. S. W. Butler and J. A. Stefani, *IEEE Trans. Semcond. Manuf.*, **7**, 193 (1994).
19. A. J. Miller, *Subset Selection in Regression*, Chapman and Hall, New York (1990).
20. G. A. F. Seber, *Multivariate Observations*, John Wiley & Sons, New York (1984).
21. M. A. Efroymson, *Multiple Regression Analysis*, pp. 191-203, John Wiley & Sons, New York (1960).
22. J. W. Tukey, *Biometrics*, **5**, 232 (March 1949).
23. M. S. Le, T. H. Smith, D. S. Boning, and H. H. Sawin, in *Process Control, Diagnostics, and Modeling in Semiconductor Manufacturing*, M. Meyyappan, D. J. Economou, and S. W. Butler, Editors, PV 97-9, p. 3, The Electrochemical Society Proceedings Series, Pennington, NJ (1997).
24. K. Wong, D. S. Boning, H. H. Sawin, S. W. Butler, and E. M. Sachs, *J. Vac. Sci. Technol. A*, **15**, 1403 (1997).
25. D. S. Boning, J. L. Claman, K. Wong, T. J. Dalton, and H. H. Sawin, in *Proceedings of the 1994 American Control Conference*, Vol. 1, p. 897, IEEE, New York, June 1994.
26. S. Shannon, J. P. Holloway, and M. L. Brake, *J. Vac. Sci. Technol. A*, **17**, 2703 (1999).